A Computational Characterization of Boron−Oxygen Multiple Bonding in HN=CH−CH=CH−NH−BO

Joseph D. Larkin,*,†,⊥ Krishna L. Bhat,# George D. Markham,§ Tony D. James,+ Bernard R. Brooks,⊥ and Charles W. Bock‡,§

Department of Chemistry, Bloomsburg University of Pennsylvania, Bloomsburg, Pennsylvania 17815, Department of Chemistry and Biochemistry, School of Science and Health, Philadelphia University, School House Lane and Henry Avenue, Philadelphia, Pennsylvania 19144, The Institute for Cancer Research, Fox Chase Cancer Center, 7701 Burholme Avenue, Philadelphia, Pennsylvania 19111, National Heart, Lung, and Blood Institute, The National Institutes of Health, Building 50, Bethesda, Maryland 20851, Department of Chemistry, Widener University, Chester, Pennsylvania 19013, and Department of Chemistry, University of Bath, Bath BA2 7AY, U.K.

Received: January 7, 2008; Revised Manuscript Received: June 3, 2008

Structures, relative energies, and bonding characteristics for various conformers of 3-imino-*N*-(oxoboryl)prop-1-en-1-amine, HN=CH−CH=CH−NH−BO, and the corresponding borocycle (−HN=CH−CH=CH−NH−B−)O are discussed using results from second-order Møller−Plesset (MP2) perturbation theory with the Dunning−Woon correlation-consistent cc-pVDZ, aug-cc-pVDZ, and cc-pVTZ basis sets. These MP2 results are compared to those from computationally efficient density functional theory (DFT) calculations using the LDA, PBE, TPSS, BLYP, B3LYP, BVP86, OLYP, O3LYP, and PBE1PBE functionals in conjunction with the economical Pople-type 6-311++G(d,p) basis set to evaluate the suitability of these DFT/6-311++G(d,p) levels for use with larger boron-containing systems. The effects of an aqueous environment were incorporated into the calculations using COSMO methodology. The calculated boron−oxygen bond lengths, orbital compositions, and bond orders in all the (acyclic) HN=CH−CH=CH−NH−BO conformers were consistent with the presence of a boron−oxygen triple bond, similar to that found in H−B≡O and H_2N−B≡O. The (−HN=CH−CH=CH−NH−B−)O borocycle is predicted to be planar (C_{2v} symmetry), and it is ∼30 kcal/mol lower in energy than any of the (acyclic) HN=CH−CH=CH−NH−BO conformers; the boron−oxygen bond in this borocycle has significant double bond character, a bonding scheme for which there has been only one experimental structure reported in the literature (Vidovic, D.; et al. *J. Am. Chem. Soc.* 2005, *127*, 4566−4569).

Introduction

The chemistry of borates rivals that of the silicates and phosphates in terms of variation and complexity.[1] Indeed, the importance of boron derivatives in chemistry,[2,3] biochemistry,[4,5] medicinal chemistry,[6–10] and material science[11–15] is increasing rapidly, and advancing the understanding of boron bonding continues to be an important topic among chemists.[16,17] The boron−oxygen single bond in tricoordinated boronic acids (1.35−1.38 Å) and esters (1.31−1.35 Å)[3] is quite strong, ∼120 kcal/mol;[3] not surprisingly, single bond lengths in tetracoordinated species are significantly longer (1.43−1.47 Å), and there is an associated loss in bond strength (by as much as 12 kcal/mol).[3] Compounds containing boron−oxygen double bonds, that is, oxoboranes (R−B=O), have been invoked as reactive intermediates for some time,[18] but they have defied most attempts at isolation and characterization;[18–23] the oxophilicity of boron makes the formation of a B−O−B linkage more facile than formation of a boron−oxygen multiple bond.[16,17] Recently, however, Vidovic et al.[24] reported the synthesis of a novel borocycle, LBO → $AlCl_3$ (where L is a chelating β-diketiminate {$HC(CMe)_2(NC_6F_5)_2$}$^-$), in which the boron−oxygen bond was stabilized with a Lewis acid ($AlCl_3$). LBO → $AlCl_3$ had significant double bond character; for example, single-crystal X-ray diffraction data collected at 153 K showed that the boron−oxygen bond length in this borocycle was 1.304(2) Å compared to 1.354(5)−1.365(4) Å[25,26] in singly bonded N_2B−O fragments (diaza- and triazaboroles). Furthermore, calculations in vacuo performed by the same authors at the B3LYP/6-311+G(d) computational level on a (−N(C_6F_5)=C(CH_3)−CH=C(CH_3)−N(C_6F_5)−B−)O borocycle (in the absence or in the presence of a $AlCl_3$ moiety) indicated that the boron−oxygen functionality in this structure was also predominantly double-bonded. However, ongoing computational studies of boron compounds have raised concerns regarding the extent to which the popular B3LYP functional using split-valence Pople-type basis sets adequately describes some aspects of boron bonding,[27–30] suggesting that more rigorous calculations are required to confirm the Vidovic et al.[24] results.

Our particular interest in oxoboranes stems from the results of our recent computational investigation[29] of several (neutral) reaction mechanisms for the protodeboronation (hydrolysis) of BoroGlycine, H_2N−CH_2−$B(OH)_2$

* To whom correspondence should be addressed. Telephone: (570) 389-4154. E-mail: jlarkin@bloomu.edu.
† Bloomsburg University of Pennsylvania.
⊥ The National Institutes of Health.
Widener University.
§ Fox Chase Cancer Center.
+ University of Bath.
‡ Philadelphia University.

10.1021/jp800125p CCC: $40.75
Published on Web 08/15/2008

$$H_2O + H_2N{-}CH_2{-}B(OH)_2 \rightarrow B(OH)_3 + H_2N{-}CH_3 \quad (1)$$

and for the 1,2-carbon-to-nitrogen shift of the $-B(OH)_2$ moiety

$$H_2N{-}CH_2{-}B(OH)_2 \rightarrow H_3C{-}NH{-}B(OH)_2 \quad (2)$$

Surprisingly, a species of the form $H_3C{-}NH_2{-}B(OH)(=O)$, in which the boron−oxygen double bond was stabilized by a water molecule, proved to be an intermediate in the 1,2-rearrangement mechanism, leading to this study of boron−oxygen multiple bonding.

In this article, we report results from a computational investigation of the structures, relative energies, and boron bonding in various acyclic conformers of 3-imino-*N*-(oxoboryl)prop-1-en-1-amine, HN═CH−CH═CH−NH−BO, and the related borocycle (−HN═CH−CH═CH−NH−B−)O, which has the same cyclic backbone as the structure synthesized by Vidovic et al.[24] Conformers of HN═CH−CH═CH−NH−BO are expected to involve a boron−oxygen triple bond;[22,31−38] see Scheme 1A. Such oxoborons (R−B≡O) have been known experimentally for more than 30 years;[19,22,31,37−42] they are intermediates in the oxidation of solid borons, boranes, and other boron-based materials and release large amounts of energy when used in the synthesis of boron compounds, making them favorable candidates to be employed as propellants in air-breathing combusters and as rocket fuels.[33,43] Although lifetimes of these species are only ∼100 ms,[35] several small oxoboranes have been prepared, and their bonding has been characterized in the gas phase and in the solid state; experimental and computational boron−oxygen distances in such structures are relatively short,[34,41,42,44] for example, ∼1.2 Å for H−B≡O.[34,42,45]

On the other hand, the experimental and computational results reported by Vidovic et al.[24] suggest that the (−NH═CH−CH═CH−NH−B−)O borocycle is more likely to involve a boron−oxygen double bond; see Scheme 1B. Thus, a rigorous computational investigation of the model compounds HN═CH−CH═CH−NH−BO and (−NH═CH−CH═CH−NH−B−)O provides an opportunity to characterize various aspects of boron−oxygen multiple bonding within a consistent molecular framework.[5,46,47]

Computational Methods

Equilibrium geometries for the structures described in this article were obtained using second-order Møller−Plesset (MP2) perturbation theory[48] with the frozen core (FC) option, which neglects core−electron correlation; the Dunning−Woon correlation-consistent (cc) basis sets, cc-pVDZ, aug-cc-pVDZ, and cc-pVTZ, were employed for the majority of the computations.[49−52] Frequency analyses were performed analytically to confirm that the optimized structures were local minima on the PES and to correct reaction enthalpies and free energies to 298 K. The gas-phase calculations were carried out using the GAUSSIAN 03 suite of programs.[53] Bonding was analyzed with the aid of natural bond orbitals (NBOs).[54−57]

Calculations using MP2 methodology with cc basis sets are not currently practical for investigations of the larger boron derivatives of primary chemical interest. Density functional theory (DFT) with Pople-style basis sets[58,59] provide an economical alternative, but the reliability of specific functional/basis set combinations for describing the incredibly diverse range[1] of boron chemistry has yet to be fully established.[27−30] Thus, our MP2/cc results were compared to those from several more computationally efficient DFT/6-311++G(d,p) levels using the following functionals: LDA(SVWN5);[60] BLYP and B3LYP, which incorporate the dynamical functional of Lee, Yang, and Parr (LYP),[61] coupled with Becke's pure DFT exchange functional (B);[62] BVP86, which uses Perdew's 1986 functional[63,64] with local correlation replaced by that suggested by Vosko et al. (VWN);[60] OLYP[65] and O3LYP,[66] which were constructed from the novel OPTX exchange functional; PBE1PBE,[67,68] which makes use of the one-parameter generalized-gradient approximation (GGA) PBE functional[69] with a 25% exchange and 75% correlation weighting; and TPSS, the nonempirical meta-generalized gradient approximation (MGGA) functional recently developed by Staroverov, Scuseria, Tao, and Perdew.[70]

Results from continuum solvation models were employed to assess the effects of a bulk aqueous environment on the gas-phase results;[71] such continuum models only provide a description of long-range interactions and have significant limitations in describing protic solvents.[72,73] Thus, in some cases, explicit water molecules were used to provide a description of the short-range/site-specific effects of an aqueous environment. The conductor-like screening model (COSMO), pioneered by Klamt and co-workers,[74−77] was employed for the continuum calculations in an aqueous medium using the PQS ab initio program package 3.2 on a PQS Quantum Cube;[78] we employed the default settings in the COSMO module of this software which were specifically tailored to COSMO theory[76,77] and optimized for the BVP86 functional, that is, the BP86 functional[63,64] in which local correlation was replaced by VWN,[60] using the svp- and tzvp (Ahlrichs) basis sets.[79,80] These COSMO results were also compared to the corresponding gas-phase results using natural resonance theory (NRT).[54−57]

SCHEME 1

NH═CH−CH═CH−NH−B≡O **A**

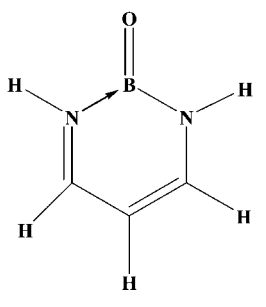

B

Results and Discussion

Since no experimental data are currently available for any conformers of HN═CH−CH═CH−NH−BO or for (−NH═CH−CH═CH−NH−B−)O, we initially considered H−BO ($C_{\infty h}$) and $H_2N{-}BO$ (C_s) at a variety of computational levels to establish "baseline" structural and bonding parameters.

A.1. H−BO and H_2N−BO. A significant amount of experimental[22,31−38,42] and computational data[33,45,81−87] has been reported in the literature for hydroboron monoxide, H−BO, an intermediate/byproduct of a variety of reactions involving boron compounds.[88] Calculated bond lengths of H−BO at the MP2(FC)/cc-pVDZ, MP2(FC)/aug-cc-pVDZ, and MP2(FC)/cc-pVTZ levels are shown in Figure 1, and vibrational frequencies at the MP2(FC)/aug-cc-pVDZ level are listed in Table 1S of the Supporting Information. Structural parameters at a variety of more-rigorous computational levels are given in Table 2S (including selected results that incorporate core−electron correlation (FULL),[53,89,90] which has virtually no effect on the calculated geometrical parameters); the analogous structural parameters at several DFT/6-311++G(d,p) levels are shown

MP2(FC)/cc-pVDZ
MP2(FC)/aug-cc-pVDZ
MP2(FC)/cc-pVTZ

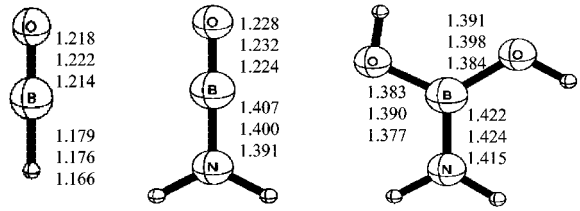

Figure 1. Optimized structures of HBO, H_2NBO, and $H_2NB(OH)_2$ (distances are in Å).

in Table 3S. The calculated boron−oxygen bond lengths, 1.218, 1.222, and 1.214 Å at the MP2(FC)/cc-pVDZ, MP2(FC)/aug-cc-pVDZ, and MP2(FC)/cc-pVTZ levels, respectively, all overestimate this length compared to that obtained from microwave spectroscopy, 1.2007 ± 0.0001 Å;[34,41,42,44] indeed, as shown by DeYonker et al.,[45] quite sophisticated computational methodology and large basis sets are required to systematically approach the microwave result. NBOs[54–57] for H−BO at the MP2/cc-pVDZ, MP2/aug-cc-pVDZ, and MP2/cc-pVTZ levels consistently showed the presence of one σ- and two π-boron−oxygen bonding orbitals. NRT[54–57] calculations with the BVP86 functional using the tzvp(svp) basis sets[60,63,64,79,80] found the boron−oxygen bond order to be ∼3.00 in H−BO, consistent with the presence of a B≡O bond; the NRT-derived covalent/ionic contributions to the total bond order were 1.24/1.76 at the BVP86/tzvp level; the Löwdin bond order[91–93] for the boron−oxygen bond in H−BO was also calculated and found to be slightly lower, 2.80(2.86), at the BVP86/tzvp(svp) levels; see Table 4S. We also list in Table 4S selected covalent bond orders derived from the atomic overlap matrix (AOM) using the Bader[94] atoms-in-molecules (AIM) approach to the analysis of electron density.[95–97]

One measure of the energy content stored in the boron−oxygen triple bond of R−B≡O monomers can be obtained from the thermochemical parameters for its trimerization to the heteroaromatic ring ($R_3B_3O_3$) boroxine structure.[35,98–100] The calculated values of ΔH^0_{298} for the conversion of hydroboron monoxide to $H_3B_3O_3$ (D_{3h}) are extremely exothermic, −91.1 and −93.2 kcal/mol in vacuo at the MP2(FC)/cc-pVDZ and MP2(FC)/aug-cc-pVDZ levels, respectively. The calculated boron−oxygen bond lengths in this boroxine are all the same, for example, 1.388 Å at the MP2(FC)/cc-pVDZ level and 1.394 Å at the MP2(FC)/aug-cc-pVDZ level, nearly 0.2 Å longer than the corresponding values in H−B≡O. The calculated NRT BVP86/svp boron−oxygen bond order in $H_3B_3O_3$ was 1.46 (0.45/1.01), only about 50% of the corresponding value in H−B≡O, suggestive of significant electron delocalization.[91,98] The Löwdin bond order was 1.45 at this level, in good agreement with the NRT value; see Table 4S.

In COSMO aqueous media[76,77] at the BVP86/tzvp level, the boron−oxygen bond length of H−B≡O increased from the corresponding gas-phase value but only by ∼0.005 Å; the boron−oxygen bond order, 3.00 (1.16/1.84), remained essentially the same. Thus, there appears to be relatively little difference in the geometrical structure or in the bonding of H−B≡O as a result of any long-range effects of bulk solvation. The calculated values of ΔH^0_{298} for the conversion of hydroboron monoxide to boroxine in COSMO aqueous media at the BVP86/tzvp level was −92.0 kcal/mol compared to −99.3 kcal/mol in vacuo at this level. To assess short-range/site-specific effects of an aqueous environment, we microsolvated the optimized MP2(FC)/cc-pVDZ gas-phase structure of H−B≡O with a few explicit water molecules initially positioned in the vicinity of the B≡O moiety. Although an exhaustive search of all possible conformers of these complexes was not practical at this level, several distinct stable structures were located for 2- and 3-water cases. The lowest-energy forms we found in these hydrated complexes involved an oxygen atom of one of the water molecules effectively bound to the boron atom in H−BO; the calculated B−O_w distance was 1.68(1.67) Å, the B−O distance was 1.26(1.27) Å, and the HBO angle was 140.4°(138.5°) for the 2(3)-water complexes; see Figure 1S in the Supporting Information; thus, there is a significant change from the linear gas-phase geometry of H−B≡O upon microsolvation. As would be expected, the calculated values of ΔH^0_{298} for the formation of the lowest-energy 2(3)-water H−BO complexes were substantially exothermic, −18.8(−31.6) kcal/mol.

Since the borocycle described by Vidovic et al.[24] and the model (acyclic) HN═CH−CH═CH−NH−BO and (cyclic) (−NH═CH−CH═CH−NH−B−)O structures all involve boron−nitrogen bonds in addition to boron−oxygen bonds, we also geometry optimized aminoboron monoxide, H_2N-BO,[5] to assess the effect of a proximal boron−nitrogen bond on the boron−oxygen structural and bonding parameters. To the authors' knowledge, no experimental synthesis, isolation, or characterization of H_2N-BO, nor any rigorous computational studies of this small molecule, have been reported. The calculated boron−oxygen separation in H_2N-BO was ∼0.01 Å longer than it was in H−B≡O at the MP2(FC)/(cc-pVDZ, aug-cc-pVDZ, and cc-pVTZ) computational levels; see Figure 1. Selected structural parameters for H_2N-BO at a variety of DFT/6-311++G(d,p) computational levels are listed in Table 3S and show similar increases for the boron−oxygen distance relative to the corresponding values for H−B≡O. The NBOs of H_2N-BO still involve one σ- and two π-bonds at all of the MP2(FC)/cc levels included in this investigation. The NRT boron−oxygen bond order in H_2N-BO, 2.90 (1.19/1.71) at the BVP86/tzvp level, was only ∼3% lower than the corresponding value in H−B≡O; the corresponding Löwdin bond order, 2.61, was ∼7% lower than that in H−B≡O. Furthermore, the weighting of the resonance structure of the form H_2N═B═O, associated with the interaction of the nitrogen lone pair orbital and an antibonding boron−oxygen orbital, was only ∼9.2% at this level. Thus, in the gas phase, the boron−oxygen bond in H_2N-BO appears to be best described as a triple bond.

We also calculated thermodynamic parameters for the trimerization of aminoboron monoxide to the boroxine structure $(H_2N)_3B_3O_3$ (D_{3h});[35] the calculated values of ΔH^0_{298} in the gas phase were −134.7, −130.2 and −125.3 kcal/mol at the MP2(FC)/cc-pVDZ, MP2(FC)/aug-cc-pVDZ, and BVP86/tzvp computational levels, respectively, significantly more exothermic than that for the analogous trimerization of hydroboron monoxide. The boron−oxygen bond lengths in the product boroxine structure were all the same, 1.396 Å at the MP2(FC)/cc-pVDZ level and 1.400 Å at the MP2(FC)/aug-cc-pVDZ level, slightly longer than the corresponding values in $H_3B_3O_3$ but indicative of significant electron delocalization;[98–103] the corresponding boron−nitrogen bond lengths were 1.409 and 1.413 Å, respectively.

As might be expected, in the COSMO aqueous media model,[76,77] the calculated boron−oxygen bond length in H_2N-BO increased, but only by ∼0.01 Å at the BVP86/tzvp level compared to the analogous value in vacuo; the resulting NRT boron−oxygen bond order, 2.55 (0.98/1.57), however, suggests that in this aqueous model, the boron−oxygen bonding

in H_2N-BO is best described as intermediate between a double and triple bond. Indeed, the NRT weighting of the $H_2N{=}B{=}O$ bonded resonance structure, 41.7%, was more than four times greater than the corresponding weighting in vacuo. Micosolvation of the gas-phase structure of H_2N-BO with a few water molecules positioned at various points around the boron−oxygen functional group, followed by reoptimization of the complex, often resulted in the corresponding amino boronic acid, $H_2N-B(OH)_2$, hydrogen-bonded to the remaining water molecules. The hydration reaction

$$H_2N-B{\equiv}O + H_2O \rightarrow H_2N-B(OH)_2 \qquad (3)$$

is highly exothermic in vacuo; for example, ΔH^0_{298} is −44.2, −41.7, −46.3, and −43.0 kcal/mol at the MP2(FC)/cc-pVDZ, MP2(FC)/aug-cc-pVDZ, MP2(FC)/cc-pVTZ, and BVP86/tzvp levels, respectively. In COSMO aqueous media at the BVP86/tzvp level, ΔH^0_{298} is −34.7 kcal/mol, ∼8 kcal/mol less negative than the corresponding value in vacuo. We also located the four-membered cyclic transition state for this hydrolysis reaction in vacuo, and the value of $\Delta H^{\ddagger}$ was only +4.8 kcal/mol relative to the separated reactants at the MP2(FC)/cc-pVDZ level. The corresponding value of $\Delta H^{\ddagger}$ at the BVP86/tzvp level was predicted to be slightly lower, +2.2 kcal/mol, whereas in COSMO aqueous media, $\Delta H^{\ddagger}$ was found to be slightly higher, +5.5 kcal/mol. The calculated values of ΔH^0_{298} for the trimerization of $H_2N-B{\equiv}O$ to the corresponding boroxine structure in this COSMO aqueous medium model was −103.0 kcal/mol compared to −125.3 kcal/mol in vacuo.

The boron−nitrogen bond length in H_2N-BO was calculated to be 1.41, 1.40, and 1.39 Å in vacuo at the MP2/cc-pVDZ, MP2/aug-cc-pVDZ, and MP2/cc-pVTZ levels, respectively; see Figure 1. The NRT bond order at the BVP86/tzvp level was 1.10 (0.53/0.59), generally consistent with the presence of a boron−nitrogen single bond with ∼10% double-bond character. The calculated B−N distance decreased in COSMO aqueous medium by ∼0.05 Å at the BVP86/tzvp level, and the NRT bond order increased to 1.45 (0.61/0.84). These findings suggest that the boron−nitrogen bond in this model media is most appropriately described as intermediate between a single and double bond.

A.2. (Acyclic) HN═CH−CH═CH−NH−BO Conformers. With the above reference data on H−BO and NH_2-BO in hand, an extensive conformational search of the (acyclic) HN═CH−CH═CH−NH−BO potential energy surface (PES) at the MP2/cc-pVDZ level was performed. A variety of conformers with different cis/trans arrangements about the heavy-atom backbone were located; these conformers typically differed in energy among each other by less than ∼5 kcal/mol. Two of these conformers, **1a** and **1b,** are shown in Figure 2; **1a** (TTT) (C_s) is the lowest-energy acyclic structure we found, whereas conformer **1b** (CCT) (C_s), which is ∼3 kcal/mol higher in energy than **1a**, see Table 1, has a more "cyclic-like" structure, but the terminal nitrogen atom was intentionally oriented to eliminate any possibility of an intramolecular boron−nitrogen dative bonding interaction. Infrared vibrational frequencies of **1a** and **1b** at the MP2(FC)/aug-cc-pVDZ level are listed in Table 1S of the Supporting Information. Calculated *xyz*-coordinates for a variety of HN═CH−CH═CH−NH−BO conformers are given in Table 5S of the Supporting Information.

The calculated boron−oxygen distances for **1a** in vacuo, 1.226, 1.231, and 1.223 Å at the MP2(FC)/cc-pVDZ, MP2(FC)/aug-cc-pVDZ, and MP2(FC)/cc-pVTZ levels, respectively, see Figure 2, are nearly the same as those in $H_2N-B{\equiv}O$ at the corresponding computational levels; see Figure 1. An examination of the NBOs in **1a** at the MP2(FC)/cc-pVDZ and MP2(FC)/aug-cc-pVDZ levels confirmed the existence of a boron−oxygen σ-bonding orbital and predicted a pair of π-bonding orbitals, similar to what was found in both $H-B{\equiv}O$ and $H_2N-B{\equiv}O$. The NRT (BVP86/tzvp) bond order for **1a**, 2.91 (1.21/1.70), was almost identical to that for $H_2N-B{\equiv}O$, 2.90 (1.19/1.71), and the corresponding Löwdin bond order, 2.63, was nearly the same as that in $H_2N-B{\equiv}O$, 2.61; see Table 4S. Furthermore, the weighting of the B≡O-bonded resonance structure was ∼62.5% compared to only ∼8.4% for the B═O-bonded structure at the BVP86/tzvp level. Thus, the boron−oxygen bond in **1a** is best described as a triple bond in vacuo.

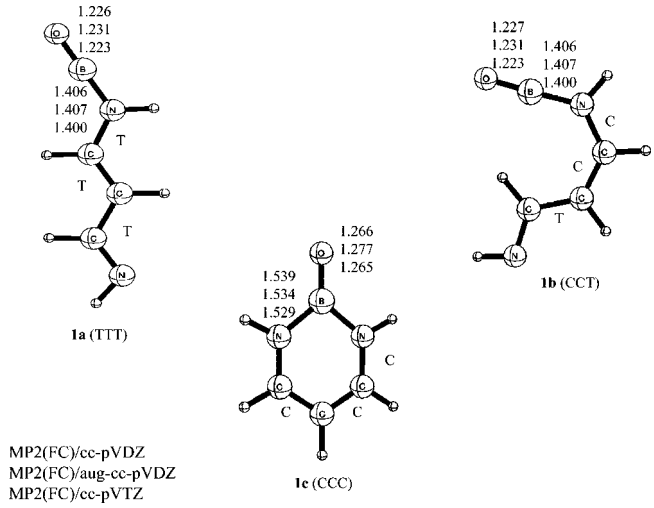

Figure 2. Optimized structures of the acyclic conformers **1a** and **1b** of HN═CH−CH═CH−NH−BO and the borocycle **1c** (−NH═CH−CH═CH−NH−B−)O (distances are in Å). AIM calculations using the MP2/cc-pVDZ density find the expected molecular graph for **1c** (12 attractors, 12 critical points on attractor interaction lines, and 1 ring point).

TABLE 1: Relative Energies, *E*(kcal/mol) (Values Thermally Corrected to 298 K in Parentheses) for the Acyclic Conformers 1a (TTT) and 1b (CCT) of NH═CH−CH═CH−NH−BO and the Cyclic Conformer 1c (CCC) of (−NH═CH−CH═CH−NH−B−)O at the MP2(FC)/cc-pVDZ, MP2(FC)/aug-cc-pVDZ, and MP2(FC)/cc-pVTZ Computational Levels

	E(kcal/mol)		
level	**1c** (CCC)	**1a** (TTT)	**1b** (CCT)
MP2(FC)/cc-pVDZ	0.0(0.0)	+31.4(+29.8)	+34.8(+33.3)
MP2(FC)/aug-cc-pVDZ	0.0(0.0)	+32.6(+31.1)	+35.3(+33.8)
MP2(FC)/cc-pVTZ	0.0(0.0)	+33.9(+32.3)	+36.9(+35.4)

Thermodynamic parameters for the conversion of **1a** to the corresponding $(NH{=}CH-CH{=}CH-NH)_3B_3O_3$ boroxine structure[42] were also computed; the calculated value of ΔH^0_{298} was −141.1 kcal/mol at the MP2(FC)/cc-pVDZ computational level compared to −134.7 kcal/mol for the analogous conversion of NH_2-BO.

In the context of the COSMO BPV86/tzvp aqueous medium model, the characteristics of the boron−oxygen bonding in all of the (acyclic) HN═CH−CH═CH−NH−BO derivatives that we investigated were similar to those that we observed for H_2N-BO; for example, the boron−oxygen distance in **1a** increased slightly, by ∼0.007 Å compared to its value in vacuo, and the NRT bond order, 2.63 (1.03/1.60), was lower than its value in vacuo, 2.91 (1.21/1.70), as was the corresponding Löwdin bond order, 2.55 compared to 2.63. Thus, the boron−oxygen bonding of NH═CH−CH═CH−NH−BO (**1a**)

in a COSMO aqueous media model appears to be intermediate between a double and triple bond.

Short-range/site-specific effects of an aqueous environment on the structure of NH═CH−CH═CH−NH−BO (**1a**) were also investigated using a few explicit water molecules initially positioned in the vicinity of the boron−oxygen moiety of the optimized gas-phase MP2(FC)/cc-pVDZ structure. An exhaustive search of all possible conformers of these complexes was obviously not possible, but a variety of different initial arrangements of the water molecules were considered; of course, this does not ensure that we obtained the global minimum on the appropriate PES. As was noted above for $H_2N-B{\equiv}O$, in some instances, these hydrated adducts of NH═CH−CH═CH−NH−BO (**1a**) (in vacuo, as well as in COSMO aqueous media) converted to the corresponding boronic acid during the reoptimization; in other adducts, the NH═CH−CH═CH−NH−BO structure remained intact, although in these conformers, the boron−oxygen bond length was relatively long, ∼1.28 Å. Indeed, the hydration reaction

$$HN{=}CH{-}CH{=}CH{-}NH{-}BO\ (\mathbf{1a}) + H_2O \rightarrow HN{=}CH{-}CH{=}CH{-}NH{-}B(OH)_2$$

was calculated to be highly exothermic; for example, ΔH^0_{298} was −49.4 and −46.4 kcal/mol at the MP2(FC)/cc-pVDZ and MP2(FC)/aug-cc-pVDZ levels, respectively, some 5 kcal/mol more exothermic than the analogous reaction for $H_2N-B{\equiv}O$. We also located the transition state for this hydration reaction in vacuo; the value of $\Delta H^{\ddagger}$ for the formation of the resulting four-membered ring structure was only +1.8 kcal/mol above the separated reactants, compared to +4.8 kcal/mol for $H_2N-B{\equiv}O$.

The boron−nitrogen bonding in **1a** is also similar to that in H_2N-BO; the compositions of the boron−nitrogen NBOs for NH═CH−CH═CH−NH−BO (**1a**) and H_2N-BO were nearly the same at the computational levels that we employed, and the calculated BVP86/tzvp NRT bond order in **1a**, 1.09 (0.49/0.60), was almost identical to that in H_2N-BO, 1.10 (0.51/0.59). The boron−nitrogen bond order for NH═CH−CH═CH−NH−BO (**1a**) in a COSMO BPV86/tzvp aqueous medium was 1.34 (0.55/0.79), attesting to the increased importance of a N═B═O resonance structure in such an environment.

A.3. (−NH═CH−CH═CH−NH−B−)O Borocycle. The (−NH═CH−CH═CH−NH−B−)O borocycle, **1c**, see Figure 2, was ∼30 kcal/mol lower in energy than any of the acyclic conformers of HN═CH−CH═CH−NH−BO that we found at the MP2/cc-pVDZ, MP2/aug-cc-pVDZ, and MP2/cc-pVTZ levels; see Table 1. Infrared frequencies of **1c**, calculated at the MP2/aug-cc-pVDZ level, are listed in Table 1S of the Supporting Information. The transition state that connects the borocycle **1c** and the acyclic conformer **1b** of HN═CH−CH═CH−NH−BO was also located; see Figure 2S of the Supporting Information. It was 40.5 and 41.0 kcal/mol higher in energy than **1c** at the MP2/cc-pVDZ and MP2/aug-cc-pVDZ levels, respectively. The calculated boron−oxygen separation in the borocycle **1c**, 1.266, 1.277, and 1.265 Å at the MP2(FC)/cc-pVDZ, MP2(FC)/aug-cc-pVDZ, and MP2(FC)/cc-pVTZ levels, respectively, is ∼0.04 Å longer than it is in the acyclic HN═CH−CH═CH−NH−BO derivatives at these levels. An examination of the NBOs in **1c** at the MP2(FC)/cc-pVDZ and MP2(FC)/aug-cc-pVDZ levels confirms the existence of a boron−oxygen σ-bonding orbital and one π-bonding orbital. The NRT boron−oxygen bond order for **1c** at the BVP86/tzvp level, 2.28 (0.95/1.33), is significantly lower than the corresponding value for the acyclic conformer, **1a**, 2.91 (1.21/1.70) at this level; the Löwdin bond order for **1c** is 2.32, compared to 2.63 for **1a** and 2.61 in $H_2N-B{\equiv}O$. Thus, in vacuo, it appears reasonable that the boron−oxygen bond in **1c** can be regarded as predominately a double bond.

In the COSMO BVP86/tzvp aqueous medium model, the length of the boron−oxygen bond in **1c** increased by ∼0.03 Å to 1.297 Å compared to its value in vacuo; the corresponding bond order decreased by ∼0.3 to 1.95 (0.72/1.23); the Löwdin bond order was only 1.50. We also optimized **1c** in the presence of two and three explicit water molecules, initially positioned in the vicinity of the BO moiety; although our computer resources only allowed a limited exploration of these PESs, the resulting $B-O_B$ distances in the reoptimized complexes tended to be relatively long, for example, ∼1.30 Å at the MP2(FC)/cc-pVDZ level. Thus, the short-range/site-specific effects of explicit water molecules on this borocycle appear to be less dramatic than those that we observed in the acyclic derivatives. Nevertheless, these findings suggest that the boron−oxygen bond in **1c** has a significant degree of double-bond character in an aqueous environment.

The calculated value of ΔH^0_{298} for the hydration reaction

$$(-NH{=}CH{-}CH{=}CH{-}NH{-}B-)O\ (\mathbf{1c}) + H_2O \rightarrow (-NH{=}CH{-}CH{=}CH{-}NH{-}B-)(OH)_2$$

was −32.6 kcal/mol at the MP2(FC)/cc-pVDZ level, much less exothermic than that for the hydrolysis of the acyclic structure HN═CH−CH═CH−NH−BO (**1a**) or for $H_2N-B{\equiv}O$, which is a reflection of the stability of the borocycle **1c** compared to that of **1a**. We located the transition state for this hydrolysis; the value of $\Delta H^{\ddagger}$ was +7.6 kcal/mol at the MP2(FC)/cc-pVDZ level, slightly higher than the corresponding values for $H_2N-B{\equiv}O$ (+4.8 kcal/mol) and HN═CH−CH═CH−NH−BO (**1a**) (+1.8 kcal/mol).

The two B−N bonds in this novel borocycle **1c** have the same length, that is, there is no structural distinction between the "formal" N−B single bond and the N:B dative bond, a reflection of the extent of electron delocalization in this conformer. The boron−nitrogen distances in **1c**, 1.539, 1.534, 1.529, and 1.538 Å at the MP2(FC)/cc-pVDZ, MP2(FC)/aug-cc-pVDZ, MP2(FC)/cc-pVTZ and BPV86/tzvp levels, respectively, are ∼0.13 Å longer than the corresponding boron−nitrogen separation in **1a** and **1b**.

For a more direct comparison with the experimental results of Vidovic et al.,[24] we also geometry-optimized one conformer of the $(-N(C_6F_5){=}C(CH_3){-}CH{=}C(CH_3){-}N(C_6F_5){-}B-)O$ borocycle at the MP2/cc-pVDZ level in vacuo; see Figure 3. The computed boron−oxygen bond length, 1.264 Å, was marginally shorter than the corresponding distance in NH═CH−CH═CH−NH−BO (**1c**) at this computational level but significantly shorter than the calculated value at the B3LYP/6-311+G(d) level, 1.292 Å, and even shorter than the experimental X-ray distance in the crystal structure of $(-N(C_6F_5){=}C(CH_3){-}CH{=}C(CH_3){-}N(C_6F_5){-}B-)O \rightarrow AlCl_3$, 1.304(2) Å.[24] The corresponding boron−oxygen bond length for an acyclic conformer of $N(C_6F_5){=}C(CH_3){-}CH{=}C(CH_3){-}N(C_6F_5){-}BO$ that is analogous to conformer **1a** of HN═CH−CH═CH−NH−BO was 1.226 Å at the MP2/cc-pVDZ level, slightly longer than the corresponding length in NH═CH−CH═CH−NH−BO (**1a**) but ∼0.04 Å shorter than this length in $(-N(C_6F_5){=}C(CH_3){-}CH{=}C(CH_3){-}N(C_6F_5){-}B-)O$; this (acyclic) $N(C_6F_5){=}C(CH_3){-}CH{=}C(CH_3){-}N(C_6F_5){-}BO$ conformer was 34.4 kcal/mol higher in energy than that for the analogous borocycle. The NBOs of $(-N(C_6F_5){=}C(CH_3){-}CH{=}C(CH_3){-}N(C_6F_5){-}B-)O$ indicate the presence of one σ- and only one π-boron−oxygen

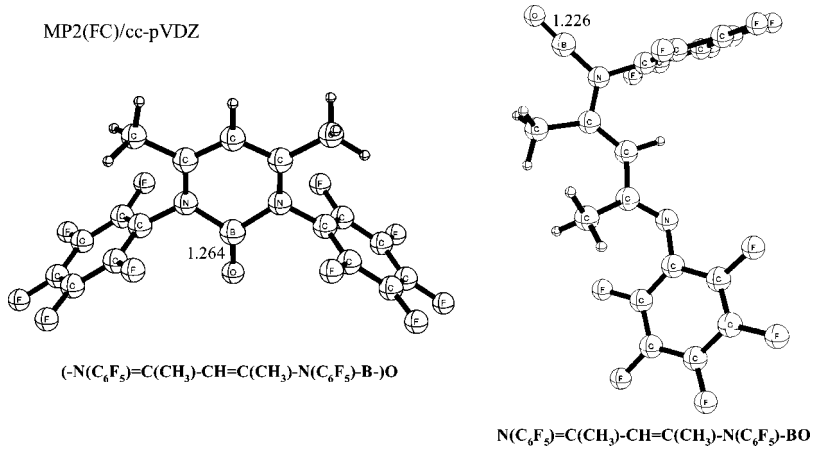

Figure 3. Optimized structures of the borocycle (−N(C_6F_5)═C(CH_3)−CH═C(CH_3)−N(C_6F_5)−B−)O and the acyclic conformer N(C_6F_5)═C(CH_3)−CH═C(CH_3)−N(C_6F_5)−BO at the MP2/cc-pVDZ computational level.

bonding orbital, suggesting the presence of a double bond, corroborating the interpretation of Vidovic et al.[24]

A.4. A Comparison of MP2(FC)/(aug)cc-pVxZ (x = D,T) and DFT/6-311++G(d,p) Results for HN═CH−CH═CH−NH−BO and (−NH═CH−CH═CH−NH−B−)O. Calculated boron−oxygen and boron−hydrogen(nitrogen) bond lengths in H−B≡O, H_2N−B≡O, H_2N−B(OH)$_2$, HN═CH−CH═CH−NH−B≡O (**1a**−**b**), and (−NH═CH−CH═CH−NH−B−)O (**1c**) are listed in Table 3S at a variety of DFT/6-311++G(d,p) levels; the Pople-style 6-311++G(d,p) basis set is at the "upper end" of basis sets that are likely to be employed in studies of larger boron-containing compounds in the near future. In this investigation, we have performed a limited comparison between the more rigorous MP2(FC) methodology using the (aug)cc-pV(D,T)Z, basis sets and the more economical DFT methodology with the LDA, PBE, TPSS, BLYP, B3LYP, BVP86, OLYP, O3LYP, and PBE1PBE functionals using the 6-311++G(d,p) basis set.

Comparing the calculated MP2/(cc-pVDZ, aug-cc-pVDZ, cc-pVTZ) boron−oxygen bond distances, see Figures 1 and 2, and the corresponding DFT/6-311++G(d,p) distances given in Table 3S, it is evident that there is reasonable agreement among these various methods/basis sets to within ∼0.02Å. The calculated boron−oxygen bond length in H−B≡O at both the B3LYP/6-311++G(d,p) and the PBE1PBE/6-311++G(d,p) levels was in particularly good agreement with the microwave data; see Table 3S. Furthermore, this finding does not appear to be highly basis-set-dependent; the boron−oxygen bond lengths calculated using the B3LYP functional with the cc-pVDZ, aug-cc-pVDZ, and cc-pVTZ basis sets were 1.203, 1.205, and 1.200 Å, respectively, and the corresponding PBE1PBE distances were 1.202, 1.204, and 1.199 Å.

Values for a variety of DFT/6-311++G(d,p) energy differences among the acyclic conformers **1a** and **1b** of HN═CH−CH═CH−NH−BO and of the borocycle (−NH═CH−CH═CH−NH−B−)O **1c** are listed in Table 6S of the Supporting Information. A comparison of Tables 1 and 6S shows that there is good agreement between the relative energies of **1a** and **1b** at the various DFT/6-311++G(d,p) and the MP2(FC)/cc levels, that is, conformer **1b** is consistently ∼3−4 kcal/mol higher in energy than **1a**. As might be expected, the variation of energy values (corrected to 298 K) between the borocycle **1c** and the acyclic conformer **1a** is significantly greater, ranging from 27.8 (B3LYP) to 42.5 kcal/mol (LDA). However, ignoring the LDA value, which includes only local terms in the correlation functional, the variation is significantly less; the highest value is 35.3 kcal/mol (PBE1PBE). The corresponding MP2(FC)/(aug)-cc-pVD(T)Z values range from 29.8 to 32.3 kcal/mol; see Table 1. Thus, to a large extent, these DFT/6-311++G(d,p) energy differences are in quite good agreement with the available MP2(FC)/cc results; unfortunately, no experimental data are currently available for comparison. In view of our previous results involving dative bonding interactions,[27–30] it appears that the PBE1PBE/6-311++G(d,p) computational level is a reasonable, economical alternative to the more-costly MP2(FC)/cc levels for exploring various aspects of boron chemistry.

It is of interest to assess geometrical and energetic results associated with climbing the DFT ladder ("Jacob's ladder"); LDA → PBE → TPSS,[104] using the modest 6-311++G(d,p) basis set. The calculated LDA/6-311++G(d,p) boron−oxygen bond length in H−B≡O, 1.202 Å, is in excellent agreement with the experimental microwave value of 1.201 Å, as well as with the corresponding B3LYP and PBE1PBE values. The initial LDA → PBE step on the ladder at this computational level results in a boron−oxygen bond length that is ∼0.01 Å longer and nearly the same as the MP2(FC)/6-311++G(d,p) length, 1.212 Å. The second step on the DFT ladder is PBE → TPSS. At this step, the boron−oxygen bond length changes minimally; see Table 3S. The energy difference between the borocycle **1c** and the acyclic derivative **1b** improves dramatically in going from LDA to PBE compared to the various MP2(FC)/cc differences and most of the DFT/6-311++G(d,p) differences; see Tables 1 and 6S. The energy change in going from PBE to TPSS is minimal.

Concluding Remarks

The importance of boron chemistry is increasing rapidly in a variety of fields, and unveiling the intricacies of boron bonding remains an active area of research.[3,17,19,24,26,29,81,82] In this article, we report results from a computational investigation of the boron−oxygen bonding in H−BO and H_2N−BO, as well as in the acyclic conformers of HN═CH−CH═CH−NH−BO (**1a**, **1b**) and in the corresponding borocycle (−NH═CH−CH═CH−NH−B−)O (**1c**); MP2 methodology with the correlation-consistent cc-pVDZ, aug-cc-pVDZ, and cc-pVTZ basis sets and DFT methodology with the 6-311++G(d,p) basis set were employed for the calculations.

Experimentally and/or computationally derived distances between the boron and oxygen atoms, a key parameter in any discussion of bond order,[105] the calculated composition of the molecular orbitals at a variety of MP2/cc and DFT/6-

311++G(d,p) levels, and the computed NRT bond orders at the BVP86/(svp)tzvp-Ahlrichs levels are consistent with the presence of a boron−oxygen triple bond in H−BO, H_2N−BO, and various (acyclic) conformers of HN═CH−CH═CH−NH−BO in vacuo. Using the COSMO BVP86/(svp)tzvp models to simulate the long-range effects of an aqueous medium, the boron−oxygen bond in H−BO was still best described as a triple bond, whereas for H_2N−BO and HN═CH−CH═CH−NH−BO (**1a**, **1b**), this bond appears to be more appropriately described as intermediate between a double and triple bond. Incorporating several explicit water molecules in the vicinity of the boron−oxygen bond during the optimization of complexes of H_2N−B≡O and HN═CH−CH═CH−NH−BO (**1a**), to account for short-range/site-specific effects on the boron−oxygen bonding, often resulted in the corresponding boronic acid, suggesting that in an aqueous environment, the presence of H_2N−B≡O or HN═CH−CH═CH−NH−BO (**1a**, **1b**) would be short-lived. The boron−nitrogen bond in H_2N−B≡O and HN═CH−CH═CH−NH−B≡O (**1a**, **1b**) was predominantly a single bond in vacuo but was predicted to have substantial double-bond character by the COSMO BVP86/tzvp aqueous media model.

At all of the MP2(FC)/(aug)-cc-pVxZ and DFT/6−311+G(*d*,*p*) computational levels that we employed in this investigation, the (−NH═CH−CH═CH−NH−B−)O borocycle, **1c** (C_{2v} symmetry), was ∼30 kcal/mol lower in energy than any of the HN═CH−CH═CH−NH−B≡O acyclic conformers that we found; see Tables 1 and 5S. All indications are that the boron−oxygen bond in this borocycle is predominantly a double bond, in accord with the available experimental results on (−N(C_6F_5)═C(CH_3)−CH═C(CH_3)−N(C_6F_5)−B−)O.[24] The calculated lengths of the two boron−nitrogen bonds in **1c** and (−N(C_6F_5)═C(CH_3)−CH═C(CH_3)−N(C_6F_5)−B−)O were identical, a measure of the extent of electron delocalization in this conformer.

The hydration reactions

$$\text{HN═CH−CH═CH−NH−BO (\textbf{1a}, \textbf{1c})} + H_2O \rightarrow \text{HN═CH−CH═CH−NH−B(OH)}_2$$

were calculated to be highly exothermic; the calculated values of ΔH^0_{298} for **1a** and **1c** were −49.4 and −32.6 kcal/mol, respectively, at the MP2(FC)/cc-pVDZ level, an indication of the amount of energy stored in the boron−oxygen bond in these compounds. Furthermore, the calculated value of ΔH^0_{298} for the trimerization reaction of HN═CH−CH═CH−NH−BO (**1a**) to form the ((NH═CH−CH═CH−NH)$_3B_3O_3$) boroxine structure was −141.1 kcal/mol at the MP2(FC)/cc-pVDZ computational level. These findings help to quantify the high-energy content of BO multiple bonds.

Acknowledgment. This research was supported, in part, by the Intramural Research Program of the NIH, NHLBI. K.L.B. would like to thank the National Textile Center (C03-PH01); G.D.M. would like to thank NIH (GM31186, CA06927) and NCI for financial support of this work, which was also supported by an appropriation from the Commonwealth of Pennsylvania. The High Performance Computing Facility at the Fox Chase Cancer Center was used for some of the calculations described in this manuscript.

Supporting Information Available: Additional theoretical results. This material is available free of charge via the Internet at http://pubs.acs.org.

References and Notes

(1) Li, Q.; Xue, F.; Mak, T. C. W. Crystalline inclusion compounds of urea with oxoboron components. Stabilization of the elusive dihydrogen borate anion in a hydrogen-bonded host lattice. *Inorg. Chem.* **1999**, *38*, 4142–4145.

(2) Ali, H. A., Dembitsy, V., Srebnic, M. *Contemporary Aspects of Boron Chemistry and Biological Applications*; Elsevier: Amsterdam, The Netherlands, 2005.

(3) Hall, D. G. *Boronic Acids: Preparation and Applications in Organic Synthesis and Medicine*; John Wiley and Sons, Inc.: New York, 2005.

(4) Blacquiere, J. M.; Sicora, O.; Vogels, C. M.; Cuperlovic-culf, M.; Decken, A.; Ouellette, R. J.; Westcott, S. A. Dihydropyrimidinones containing boronic acids. *Can. J. Chem.* **2005**, *83*, 2052–2059.

(5) Malde, A. K.; Khedkar, S. A.; Coutino, E. C. The B(OH)−NH analog is a surrogate for the amide bond (CO−NH) in peptides: an *ab initio* study. *J. Chem. Theory Comput.* **2007**, *3*, 619–627.

(6) Adams, J.; Behnke, M.; Chen, S.; Cruickshank, A. A.; Dick, L. R.; Grenier, L.; Klunder, J. M.; Ma, Y. T.; Plamondon, L.; Stein, R. L. Potent and selective inhibitors of the proteasome: dipeptidyl boronic acids. *Bioorg. Med. Chem. Lett.* **1998**, *8*, 333–338.

(7) Labutti, J.; Pearsons, I.; Huang, R.; Miwa, G.; Gan, L.-S.; Daniels, J. S. Oxidative deboronation of the peptide boronic acid proteosome inhibitor bortezomib: contributions from reactive oxygen species in this novel cytochrome P450 reaction. *Chem. Res. Toxicol.* **2006**, *19*, 539–546.

(8) Paramore, A.; Frantz, S. Fresh from the pipeline: Bortezomib. *Nat. Rev. Drug Discovery* **2003**, *2*, 611–612.

(9) Baker, S. J.; Zhang, Y. K.; Akama, T.; Lau, A.; Zhou, H.; Hernandez, V.; Mao, W.; Alley, M. R. K.; Sanders, V.; Plattner, J. J. Discovery of a new boron-containing antifungal agent, 5-fluoro-1,3-dihydro-1-hydroxy-2,1-benzoxaborole (AN2690), for the potential treatment of onychomycosis. *J. Med. Chem.* **2006**, *49*, 4447–4450.

(10) Yinghuai, Z.; Widjaja, E.; Sai, S. L. P.; Zhan, W.; Capenter, K.; Maguire, J. A.; Hosmane, N. S.; Hawthorne, M. F. Ruthenium(0) nanoparticle-catalyzed isotope exchange between 10B and 11B nuclei in decaborane(14). *J. Am. Chem. Soc.* **2007**, *129*, 6507–6512.

(11) Abrahams, B. F.; Haywood, M. G.; Robson, R. Guanidinium ion as a symmetrical template in the formation of cubic hydrogen-bonded borate networks with the boracite topology. *J. Am. Chem. Soc.* **2005**, *127*, 816–817.

(12) Li, Y.; Ruoff, R. S.; Chang, R. P. H. Boric acid nanotubes, nanotips, nanorods, microtubes, and microtips. *Chem. Mater.* **2003**, *15*, 3276–3285.

(13) Parry, P. R.; Wang, C.; Batsanov, A. S.; Bryce, M. R.; Tarbit, B. Functionalized pyridylboronic acids and their Suzuki cross-coupling reactions to yield novel heteroarylpyridines. *J. Org. Chem.* **2002**, *67*, 7541–7543.

(14) Wang, W.; Zhang, Y.; Huang, K. Prediction of a family of cage-shaped boric acid clusters. *J. Phys. Chem. B* **2005**, *109*, 8562–8564.

(15) Wang, W. J.; Zhang, Y.; Huang, K. Self-curl and self-assembly of boric acid clusters. *Chem. Phys. Lett.* **2005**, *405*, 425–428.

(16) Nguyen, M. T.; Ruelle, P. Comparative SCF study of the nature of the carbon-phosphorous bond in phospha-alkynes, RCP, and of the boron−sulphur bond in sulphidoborons, RBS. *J. Chem. Soc., Faraday Trans.* **1984**, *2*, 1225–1234.

(17) Walawalkar, M. G. Multiple bonds continue to fascinate chemists: discovery of stable Si≡Si and B═O bonds. *Curr. Sci.* **2005**, *89*, 606–607.

(18) Pachaly, B.; West, R. Synthesis of a 1,3-dioxa-2,4-diboretane: an oxoborane precursor. *J. Am. Chem. Soc.* **1985**, *107*, 2987–2988.

(19) Groteklaes, M.; Paetzold, P. Oxo(tri-*tert*-butylphenyl)boran ArBO als Zwischenstufe. *Chem. Ber.* **1988**, *121*, 809–810.

(20) Hanecker, E.; Nöth, H.; Wietelmann, U. Beiträge zur Chemie des Bors, 171. Kristall- und Molekülstruktur von 2,4-Bis(2,2,6,6-tetramethylpiperidino)-1,3,2,4-dichalcogendiboretanen. *Chem. Ber.* **2006**, *119*, 1904–1910.

(21) Ito, M.; Tokitoh, N.; Okazaki, R. A novel approach to an oxoborane and its Lewis base complex. *Tetrahedron Lett.* **1997**, *38*, 4451–4454.

(22) Paetzold, P.; Neyses, S.; Geret, L. Oxo(trisyl)boran ($ME_3SI)_3C$−BO als Zwischenstufe. *Z. Anorg. Allg. Chem.* **1995**, *621*, 732–736.

(23) Tokitoh, N.; Ito, M.; Okazaki, R. New aspects of boron-containing low-coordinate compounds. *Main Group Chem. News* **2000**, *7*, 27–36.

(24) Vidovic, D.; Moore, J. A.; Jones, J. N.; Cowley, A. H. Synthesis and characterization of a coordinated oxoborane: Lewis acid stabilization of a boron-oxygen double bond. *J. Am. Chem. Soc.* **2005**, *127*, 4566–4567.

(25) Weber, L.; Dobbert, E.; Stammler, H. G.; Neumann, B.; Boese, R.; Blaser, D. Reaction of 1,3-dialkyl-4,5-dimethylimidazol-2-ylidenes with 2-bromo-2,3-dihydro-1H-1,3,2-diazaboroles (alkyl equals iPr and tBu). *Chem. Ber./Recl.* **1997**, *130*, 705–710.

(26) Weber, L.; Schnieder, M.; Stammler, H. G.; Neumann, B.; Schoeller, W. W. Synthesis, structure and reactivity of 3,4-dihydro-2H-1,2,4,3-triazaboroles. *Eur. J. Inorg. Chem.* **1999**, *7*, 1193–1198.

(27) Bhat, K. L.; Braz, V.; Laverty, E.; Bock, C. W. The effectiveness of a primary aliphatic amino group as an internal Lewis base on the formation of a boron−oxygen−carbon linkage: a computational study. *J. Mol. Struct.: THEOCHEM* **2004**, *712*, 9–19.

(28) Bhat, K. L.; Hayik, S.; Corvo, J. N.; Marycz, D. M.; Bock, C. W. A computational study of the formation of 1,3,2-dioxaborolane from the reaction of dihydroxy borane with 1,2-ethanediol. *J. Mol. Struct.: THEOCHEM* **2004**, *673*, 145–154.

(29) Larkin, J. D.; Bhat, K. L.; Markham, G. D.; Brooks, B. R.; Lai, J. H.; Bock, C. W. A computational investigation of the geometrical structures and protodeboronation of BoroGlycine, $H_2N-CH_2-B(OH)_2$. *J. Phys. Chem. A* **2007**, 6489–6500.

(30) Larkin, J. D.; Milkevitch, M.; Bhat, K. L.; Markham, G. D.; Brooks, B. R.; Bock, C. W. Dimers of boroGlycine and methylamine boronic acid: A computational comparison of the relative importance of dative *versus* hydrogen bonding. *J. Phys. Chem.* **2007**, *112*, 125–133.

(31) Bock, H.; Cederbaum, L.; von Niessen, W.; Paetzold, P.; Rosmus, P.; Solouki, B. Methylboron oxide, H_3C-BO. *Angew. Chem., Int. Ed.* **2003**, *28*, 88–90.

(32) Brown, R. C.; Kolb, C. E.; Yetler, R. A.; Dryer, F. L.; Rabitz, H. R. *Development of a boron assisted combustion model with sensitivity analysis*; Report prepared for the United States Air Force, Office of Scientific Research; March **1987**.

(33) Garland, N. L.; Stanton, C. T.; Nelson, H. H. Temperature dependence of the kinetics of the reaction $BO + H_2 \rightarrow HBO + H$. *J. Chem. Phys.* **1991**, *95*, 2511–2515.

(34) Kawashima, Y.; Endo, Y.; Hirota, E. Microwave spectrum, molecular structure, and force field of HBO. *J. Mol. Spectrosc.* **1989**, *133*, 116–127.

(35) Kawashima, Y.; Kawaguchi, K.; Hirota, E. Detection of HBO by discharge modulated diode laser spectroscopy. *Chem. Phys. Lett.* **1986**, *131*, 205–208.

(36) Larson, J. W.; McMahon, T. B. Gas phase bihalide and pseudo-bihalide ions. An ion cyclotron resonance determination of hydrogen bond energies in XY^- species(X,Y = F, Cl, Br, CN). *Inorg. Chem.* **1984**, *23*, 2029–2033.

(37) Lory, E. R.; Porter, R. F. Infrared spectrum of matrix-isolated HBO. *J. Am. Chem. Soc.* **1971**, *93*, 6301–6302.

(38) Snelson, A. Infrared matrix isolation spectrum of OBF. *High Temp. Sci.* **1972**, *4*, 141–146.

(39) Ault, B. S. Excimer-laser-induced oxidation of diborane: formation and isolation of HBO, $HB^{18}O$ and $H_3B_3O_3$ in argon matrices. *Chem. Phys. Lett.* **1989**, *157*, 547–551.

(40) Boyer, D. W. Shock-tube measurements of the band strengths of HBO_2 and OBF in the short wavelength infrared. *J. Quant. Spectrosc. Radiat. Transfer* **1980**, *24*, 269–282.

(41) Kawaguchi, K.; Endo, Y.; Hirota, E. Infrared diode laser and microwave spectroscopy of an unstable molecule: CIBO. *J. Mol. Spectrosc.* **1982**, *93*, 381–388.

(42) Kawashima, Y. Detection and equilibrium molecular structure of a short-lived molecule, HBO, by microwave spectroscopy. *Chem. Phys. Lett.* **1987**, *135*, 441–445.

(43) Peng, Q.; Wang, Y.; Suo, B.; Shi, Q.; Wen, Z. On the interconversion pathway of HBO<-->BOH. *J. Chem. Phys.* **2004**, *121*, 778–782.

(44) Kawashima, Y.; Kawaguchi, K.; Endo, Y.; Hirota, E. Infrared diode laser and microwave spectra and molecular structure of an unstable molecule. *J. Chem. Phys.* **1987**, *87*, 2006–2009.

(45) DeYonker, N. J.; Li, S.; Yamaguchi, Y.; Schaefer, H. F., III; Crawford, T. D.; King, R. A.; Peterson, K. A. Application of equation-of-motion coupled-cluster methods to low-lying singlet and triplet electronic states of HBO and BOH. *J. Chem. Phys.* **2005**, *122*, 234311–234313.

(46) Malde, A. K.; Khedkar, S. A.; Coutino, E. C. The stationary points of the PES of N-methoxy peptides and their boron isosteres: an *ab initio* study. *J. Chem. Theory Comput.* **2006**, *2*, 1664–1674.

(47) Zhu, L.; Shabbir, S. H.; Gray, M.; Lynch, V. M.; Sorey, S.; Anslyn, E. V. A structural investigation of the N−B interaction in an *o*-(N,N-dialkylaminomethyl)arylboronate system. *J. Am. Chem. Soc.* **2006**, *128*, 1222–1232.

(48) Møller, C.; Plesset, M. S. Note on an approximation treatment for many-electron systems. *Pure Appl. Chem.* **1934**, *46*, 618–622.

(49) Dunning, T. H. Gaussian-basis sets for use in correlated molecular calculations 0.1. The atoms boron through neon and hydrogen. *J. Chem. Phys.* **1989**, *90*, 1007–1023.

(50) Kendall, R. A.; Dunning, J. T. H.; Harrison, R. J. Electron affinities of the first-row atoms revisited. Systematic basis sets and wave functions. *J. Chem. Phys.* **1992**, *96*, 6796–6806.

(51) Peterson, K. A.; Woon, D. E.; Dunning, J. T. H. Benchmark calculations with correlated molecular wave functions. IV. The classical barrier height of the $H + H_2 \rightarrow H_2 + H$ reaction. *J. Chem. Phys.* **1994**, *100*, 7410–7415.

(52) Woon, D. E.; Dunning, T. H. Gaussian-basis sets for use in correlated molecular calculations 0.3. The atoms aluminum through argon. *J. Chem. Phys.* **1993**, *98*, 1358–1371.

(53) Frisch, M. J. Trucks, G. W.; Schlegel, H. B.; Scuseria, G. E.; Robb, M. A.; Cheeseman, J. R.; Montgomery, J. A., Jr.; Vreven, T.; Kudin, K. N.; Burant, J. C.; Millam, J. M.; Iyengar, S. S.; Tomasi, J.; Barone, V.; Mennucci, B.; Cossi, M.; Scalmani, G.; Rega, N.; Petersson, G. A.; Nakatsuji, H.; Hada, M.; Ehara, M.; Toyota, K.; Fukuda, R.; Hasegawa, J.; Ishida, M.; Nakajima, T.; Honda, Y.; Kitao, O.; Nakai, H.; Klene, M.; Li, X.; Knox, J. E.; Hratchian, H. P.; Cross, J. B.; Bakken, V.; Adamo, C.; Jaramillo, J.; Gomperts, R.; Stratmann, R. E.; Yazyev, O.; Austin, A. J.; Cammi, R.; Pomelli, C.; Ochterski, J. W.; Ayala, P. Y.; Morokuma, K.; Voth, G. A.; Salvador, P.; Dannenberg, J. J.; Zakrzewski, V. G.; Dapprich, S.; Daniels, A. D.; Strain, M. C.; Farkas, O.; Malick, D. K.; Rabuck, A. D.; Raghavachari, K.; Foresman, J. B.; Ortiz, J. V.; Cui, Q.; Baboul, A. G.; Clifford, S.; Cioslowski, J.; Stefanov, B. B.; Liu, G.; Liashenko, A.; Piskorz, P.; Komaromi, I.; Martin, R. L.; Fox, D. J.; Keith, T.; Al-Laham, M. A.; Peng, C. Y.; Nanayakkara, A.; Challacombe, M.; Gill, P. M. W.; Johnson, B.; Chen, W.; Wong, M. W.; Gonzalez, C.; Pople, J. A. *Gaussian 03*, revision B.02; Gaussian, Inc.: Pittsburgh, PA, 2003.

(54) Carpenter, J. E.; Weinhold, F. Analysis of the geometry of the hydroxymethyl radical by the "different hybrids for different spins" natural bond orbital procedure. *J. Mol. Struct.: THEOCHEM* **1988**, *169*, 41–62.

(55) Curtiss, L. A.; Weinhold, F. Intermolecular interactions from a natural bond orbital. *Chem. Rev.* **1988**, *88*, 899–926.

(56) Foster, J. P.; Weinhold, F. Natural hybrid orbitals. *J. Am. Chem. Soc.* **1980**, *102*, 7211–7218.

(57) Reed, A. E.; Weinstock, R. B.; Weinhold, F. Natural population analysis. *J. Chem. Phys.* **1985**, *83*, 735–746.

(58) Krishnan, R.; Binkley, J. S.; Seeger, R.; Pople, J. A. Self-consistent molecular-orbital methods. 20. Basis set for correlated wave-functions. *J. Chem. Phys.* **1980**, *72*, 650–654.

(59) Clark, T.; Chandrasekhar, J.; Spitznagel, G. W., III. The 3-21+G basis set for first-row elements, Li−F. *J. Comput. Chem.* **2004**, *4*, 294–301.

(60) Vosko, S. H.; Wilk, L.; Nusair, M. Accurate spin-dependent electron liquid correlation energies for local spin density calculations: a critical analysis. *Can. J. Phys.* **1980**, *58*, 1200–1211.

(61) Lee, C.; Yang, W.; Parr, R. G. Development of the Colle−Salvetti correlation-energy formula into a functional of the electron density. *Phys. Rev. B: Condens. Matter* **1988**, *37*, 785–789.

(62) Becke, A. D. Density-functional thermochemistry. 3. The role of exact exchange. *J. Chem. Phys.* **1993**, *98*, 5648–5652.

(63) Perdew, J. P. Density-functional approximation for the correlation energy of the inhomogeneous electron gas. *Phys. Rev. B* **1986**, *33*, 8822–8824.

(64) Perdew, J. P.; Zunger, A. Self-interaction correction to density-functional approximations for many-electron systems. *Phys. Rev. B* **1981**, *23*, 5048–5079.

(65) Handy, N. C.; Cohen, A. J. Left-right correlation energy. *Mol. Phys.* **2001**, 403–412.

(66) Cohen, A. J.; Handy, N. C. Dynamic correlation. *Mol. Phys.* **2001**, *99*, 607–615.

(67) Perdew, J. P.; Burke, K.; Ernzerhof, M. Generalized gradient approximation made simple (vol 77, pg 3865, 1996). *Phys. Rev. Lett.* **1997**, *78*, 1396–1396.

(68) Rabuck, A. D.; Scuseria, G. E. Assessment of recently developed density functionals for the calculation of enthalpies of formation in challenging cases. *Chem. Phys. Lett.* **1999**, *309*, 450–456.

(69) Perdew, J. P.; Burke, K.; Ernzerhof, M. Generalized gradient approximation made simple. *Phys. Rev. Lett.* **1996**, *77*, 3865–3868.

(70) Staroverov, V. N.; Scuseria, G. E.; Tao, J.; Perdew, J. P. Comparative assessment of a new nonempirical density functional: molecules and hydrogen-bonded complexes. *J. Chem. Phys.* **2003**, *119*, 12129–12137.

(71) Tomasi, J.; Mennucci, B.; Cammi, R. Quantum mechanical continuum solvation models. *Chem. Rev.* **2005**, *105*, 2999–3093.

(72) Castejon, H.; Wiberg, K. B. Solvent effects on methyl transfer reactions. 1. The Menshutkin reaction. *J. Am. Chem. Soc.* **1999**, *121*, 2139–2149.

(73) Castejon, H.; Wiberg, K. B.; Sklenak, S.; Hinz, W. Solvent effects on methyl transfer reactions. 2. The reaction of amines with trimethylsulfonium salts. *J. Am. Chem. Soc.* **2001**, *123*, 6092–6097.

(74) Andzelm, J.; Koelmel, C.; Klamt, A. Incorporation of solvent effects into density functional calculations of molecular enrgies and geometries. *J. Chem. Phys.* **1995**, *103*, 9312–9320.

(75) Baldridge, K.; Klamt, A. GAMESS/COSMO: First principle implementation of solvent effects without outlying charge error. *J. Chem. Phys.* **1997**, *106*, 6622–6633.

(76) Klamt, A. On the calculation of UV/vis-spectra in solution. *J. Phys. Chem.* **1995**, *99*, 2224–2235.

(77) Klamt, A.; Jonas, V.; Bürger, T.; Lohrenz, J. C. W. Refinement and parametrization of COSMO-RS. *J. Phys. Chem. A* **1998**, *102*, 5074–5085.

(78) *PQS Ab Initio Program* , Package 3.2; Parallel Quantum Solutions: Fayetteville, AR, 2005.

(79) Schäfer, A.; Horn, H.; Ahlrichs, R. Fully optimized contracted Gaussian basis sets for atoms Li to Kr. *J. Chem. Phys.* **1992**, *97*, 2571–2577.

(80) Schäfer, A.; Huber, C.; Ahlrichs, R. Fully optimized contracted Gaussian basis sets of triple-ζ valence quality for atoms Li to Kr. *J. Chem. Phys.* **1994**, *100*, 5829–5835.

(81) Francisco, J. S. *Ab initio* study of the structure, bonding, vibrational spectra, and energetics of XBS^+ (where X = H, F, and C1). *J. Chem. Phys.* **2006**, *124*, 114303–114310.

(82) Nguyen, M. T.; Groarke, P. J.; Ha, T.-K. Calculated properties of some oxoborons R−B≡O (R = H, F, C1 and CH_3) and their higher energy isomers R−O−B. *Mol. Phys.* **1992**, *75*, 1105–1121.

(83) Nguyen, M. T.; Vanquickenborne, L. G.; Sana, M.; Leroy, G. Heats of formation and proton affinities of some oxoborons (R−B−O) and sulfidoborons (R−B═S) with R = H, F, C1 and CH_3. *J. Chem. Phys.* **1993**, *97*, 5224–5227.

(84) Mains, G. J. Ab initio molecular orbital study of adducts and oxides of boron hydrides. *J. Phys. Chem.* **1991**, *95*, 5089–5096.

(85) Alberti, M.; Sayós, R.; Solé, A.; Aguilar, A. $B(^2P) + H_2O(X\ ^1A_1)$: a quasi-classical 3D trajectory calculation. *J. Chem. Soc., Faraday Trans.* **1991**, *87*, 1057–1068.

(86) Peterson, K. A.; Woods, R. C. Ground state spectroscopic and thermodynamic properties of AiO^-, SiN^-, CP^-, BS^-, and CN^- from Møller−Plesset perturbation theory. *J. Chem. Phys.* **1989**, *90*, 7239–7250.

(87) Talaty, E. R.; Huang, Y.; Zandler, M. E. Optimized energies and shapes ofHBO, HBS, HAIO, and HCS^+ and their isomers. *J. Am. Chem. Soc.* **1991**, *113*, 779–786.

(88) Chin, C. H.; Mebel, A. M.; Hwang, D.-Y. Theoretical study of the reaction mechanism of BO, B_2O_2, and BS with H_2. *J. Phys. Chem. A* **2004**, *1008*, 473–483.

(89) Stanton, J. F.; Gauss, J.; Lauderdale, W. J.; Watts, J. D.; Bartlett, R. J. The package also contains modified versions of the *MOLECULE Gaussian* integral program of Almlöf, J.; Taylor, P. R., the *ABACUS* integral derivative program written by Helgaker, T. U.; Jósen, P.; Taylor, P. R., and the *PROPS* property evaluation integral code of Taylor, P.R.

(90) Woon, D. E.; Dunning, T. H. Gaussian-basis sets for use in correlated molecular calculations. V. Core-valence basis-sets for boron through neon. *J. Chem. Phys.* **1995**, *103*, 4572–4585.

(91) Lowdin, P.-O. On the non-orthogonality problem connected with the use of atomic wave functions in the theory of molecules and crystals. *J. Chem. Phys.* **1950**, *18*, 365–375.

(92) Lewars, E. G. In *Computational chemistry. Introduction to the theory and applications of molecular and quantum mechanics*; Kluwer Academic Publishers: Norwell, MA, 2004; Vol. 43, pp 4979−4980.

(93) Glendening, E. D.; Weinhold, F. Natural resonance theory II. Natural bond order and valency. *J. Comput. Chem.* **1998**, *19*, 610–627.

(94) Bader, R. F. W. *Atoms in Molecules - A Quantum Theory*; Oxford University Press: Oxford, U.K., 1990.

(95) Frenking, G.; Esterhuysen, C.; Kovacs, A. Comment on the comparative use of the electron density and its Laplacian. *Chem.—Eur. J.* **2006**, *12*, 7573–7574.

(96) Matta, C. F.; Bader, R. F. W. An experimentalist's reply to "What is an atom in a molecule". *J. Phys. Chem. A* **2006**, *110*, 6365–6371.

(97) Parr, R. G.; Nalewajski, R. F.; Ayers, P. W. What is an atom in a molecule. *J. Phys. Chem. A* **2005**, *109*, 3957–3959.

(98) Doerksen, R. J.; Thakkar, A. J. Bond orders in heteroaromatic rings. *Int. J. Quantum Chem.* **2002**, *90*, 534–540.

(99) Greig, L. M.; Karinki, B. M.; Habershon, S.; Spencer, N.; Johnston, R. L.; Harris, K. D. M.; Philp, D. Solid-state and solution phase reactivity of 10-hydroxy-10.9-boroxopenanthrene: a model building block for self-assembly processes. *New J. Chem.* **2002**, *26*, 701–710.

(100) Greig, L. M.; Slawin, A. M. Z.; Smith, M. H.; Philp, D. The dynamic covalent chemistry of mono and bifunctional boroxoaromatics. *Tetrahedron Lett.* **2007**, *63*, 2391–2403.

(101) George, P.; Bock, C. W.; Trachtman, M. Empirical resonance energies for benzene and pyridine. *Tetrahedron Lett.* **1985**, *26*, 5667.

(102) George, P.; Trachtman, M.; Bock, C. W.; Brett, A. M. An alternative approach to the problem of assessing stabilization energies in cyclic conjugated hydrocarbons. *Theor. Chim. Acta* **1975**, *38*, 121.

(103) George, P.; Trachtman, M.; Bock, C. W.; Brett, A. M. Homodesmotic reactions for the assessment of stabilization in benzenoid and other conjugated cycle hydrocarbons. *J. Chem. Soc., Perkin Trans.* **1976**, *2*, 1222.

(104) Tao, J.; Perdew, J. P.; Staroverov, V. N.; Scuseria, G. E. Climbing the density functional ladder: nonempirical meta-generalized approximation for molecules and solids. *Phys. Rev. Lett.* **2003**, *91*, 146401–146404.

(105) Power, P. P. Boron-phosphorous compounds and multiple bonding. *Angew. Chem., Int. Ed. Engl.* **1990**, *29*, 449–460.

JP800125P